

LOBATE DEBRIS APRON AND LINEATED VALLEY FILL AROUND TANAICA MONTES, MARS: IMPLICATIONS FOR LATE AMAZONIAN GLACIAL ACTIVITY IN THE REGION. Rishitosh K. Sinha, S. Vijayan and Rajiv R. Bharti, Physical Research Laboratory, Ahmedabad 380009, India (rishitosh@prl.res.in)

Introduction: Extensive glacial conditions during the Late Amazonian has been inferred from widespread identification and mapping of classical lobate debris apron (LDA)/lineated valley fill (LVF) units on Mars [1,2]. Subsurface analysis of these units using the shallow radar (SHARAD on board MRO spacecraft) sounding data has revealed presence of buried ice preserved in their subsurface [3,4]. In addition, crater size-frequency distribution plots and superposition relationships have indicated that these units probably formed during the past ~100 Ma – 1 Ga [1].

In the recent survey of ice-related flow features within the mid-latitudes, LDA/LVF units have been inferred for the first time from Tanaica Montes region (39.55° N, 269.17° E) [5,6]. Detailed characterization of LDA and LVF units identified in this region is awaited despite several studies. This is essential for understanding the processes that led to form LDA/LVF units around an isolated montes topographic setting, which is located far away from the dichotomy boundary regions (e.g. Deuteronilus Mensae) wherein classical LDA/LVF units are emplaced [1,2].

This study: We focus on conducting geomorphic, topographic and radar based observation of LDA/LVF units mapped within Tanaica Montes. This is primarily to decipher: (1) flow pattern of LDA/LVF units, (2) episodes of debris-covered glaciation, (3) probable timing of glaciation and (4) extent of buried ice preserved in this region.

Study Region: The spatial extent of study region is ~10,000 km² (Fig.1). It is surrounded by low-lying area (~1 km) in the north, which consists of fissures and grabens (e.g. Tantalus Fossae). Narrow and long depressions are apparent along the east that dissect the elevated (~1 km) landmass (e.g. Ascuris Planum and Tempe Terra). Preliminary morphological mapping of study region has ascribed them as rough, hilly material that somewhat looks like basement complex and older fractured material [7]. Within the USGS geologic map of the western equatorial region of Mars (IMAP 1802-A), Tanaica Montes is referred as an example of undifferentiated material characterized by complex structures and typical relief [7]. More recently, irregular knobs, mesas tens of kilometers across, and debris aprons extending up to tens of kilometers have been mapped within the study region [8]. Overall, the topographic flanks within the study region are steep (slope: ~6°-32°) and elevated at ~0.8-2 km, and tend to elongate in varying extents from ~20-100 km length to ~1-

20 km width. This distinct topographic setting reflects significant erosion of the interior portions.

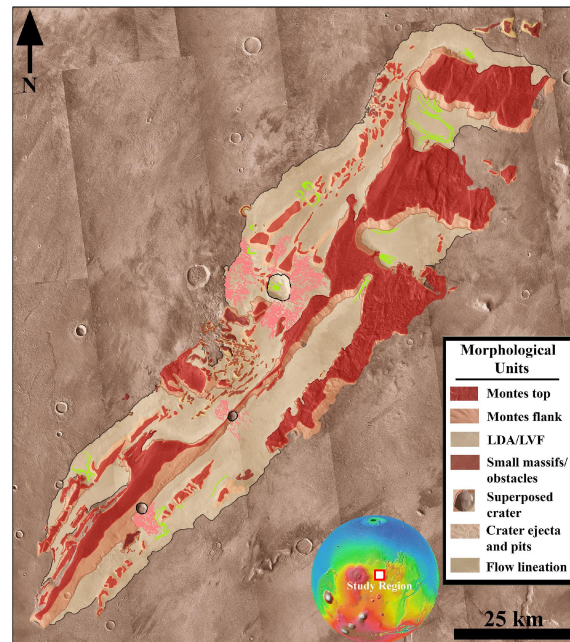


Figure 1. Morphologic map of the study region based upon MRO CTX images. LDA/LVF units are extensive. Extent of other morphological units is illustrated in the map. Location of study region is shown in the global MOLA based topographic map (red box).

Observations and Inferences: *Morphological mapping.* Multiple occurrences of integrated systems of LDA/LVF units are observed in MRO CTX images (~6 m/pixel) [9], likely resulting from downslope flow and merging of multiple lobes and layers into the surrounding plains (Fig. 1). From the upper portions of montes, multiple LDA merging and distorting downslope to become LVF flow lineations are apparent. Morphological mapping of these LDA/LVF units reveal their (1) distribution and stratigraphic relationships, (2) confined flow characteristic, and (3) flow away from the flanks base upto ~15 km. Geomorphic units resulting from (1) interaction of LDA/LVF with superposed crater's ejecta, and (2) episodic flow in the interior of these superposed craters are apparent.

Flow pattern and integration of LDA/LVF units. The flow lineations show highly integrated pattern of convergence and divergence while continuing to flow in the downslope, between the gaps in the eroded portions of montes. As such, the overall flow pattern is controlled by the underlying topography and the em-

placed lobe could be a single entity formed from coalescing of multiple flow lines, similar to typical LDA/LVF glacial systems. The integrated LDA/LVF system includes (1) accumulation of ice over montes flanks and within alcoves, (2) downslope convergence and divergence of flow ridges and lineations, (3) coalescing of flow lineations, (4) multiple flows extending away from the base of montes flank, (5) flow wrapping around and/or over obstacles, and (6) downslope convergence of flow units to emplace lobate flow features.

Topography of LDA/LVF units. The LDA/LVF units mapped within the study region tend to have moderate slope (1° - 4°) and exhibit a typical convex-up shape in MGS MOLA point tracks digitized from the base of montes flanks to outlying non LDA/LVF plains [10,11]. Intriguing relationships of LDA/LVF units with the topographic obstacles are apparent in form of (1) obstacles controlling the extent of flow and diverting the flow, and (2) flows around/over the obstacles.

Superposed LDA/LVF units. Superposed LVF lobes sourced from small alcoves are evident along the middle portion of montes flanks facing towards west. A crater emplaced over the montes flank in the lower portion of the montes surface has preserved evidence for multiple LVF flow units. These flow units have terminated in topographic lows as lobe-shaped feature.

Superposed crater ejecta and LDA/LVF units. The ejecta from at least three impact craters have superposed over the LDA/LVF units, resulting into formation of pitted units that exhibit a degraded morphology and display a range of shapes (circular to elongate) and scales (hundreds of meters to a kilometer).

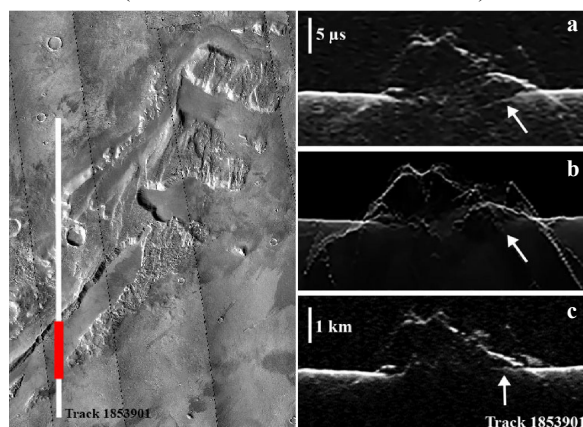


Figure 2. SHARAD observation ground-track (1853901) (white solid line) across the mapped LDAs. The base map is CTX mosaic. (a) The arrow indicates the location (red solid line in left panel) of subsurface reflector detected in the radargram. (b) Simulated radargram do not show the presence of detected subsurface reflector (as indicated by arrow). (c) The reflector becomes closely coplanar with the adjacent surface on

assuming a real dielectric constant of 3.2 (water ice) in the depth-corrected radargram (as indicated by arrow).

Subsurface of LDA/LVF units. The SHARAD based subsurface reflectors detected across the mapped LDA units reveal present-day thick ice deposits preserved in the subsurface (depth: \sim 300-500 m) (Fig. 2).

Timing of flow. From count of 727 craters on all the mapped LDA/LVF units (area: \sim 2880 km²), we estimate the modeled crater retention age to be \sim 100-700 Ma for crater diameters between 140-588 m (Fig. 3) [12]. The morphologies of counted craters vary as fresh bowl-shaped, infilled and ring-mold craters.

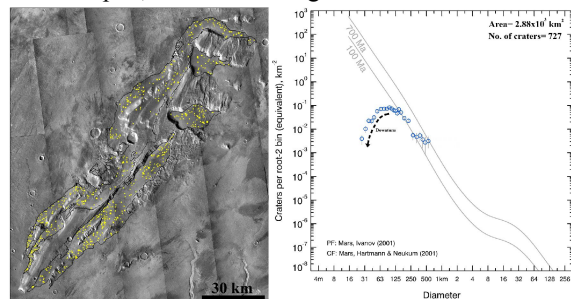


Figure 3. Crater-size frequency distribution plot for counted craters (yellow circles in the left panel). The modeled crater retention age is \sim 100-700 Ma [12]. The downturn is suggestive of a period of resurfacing.

Summary and Conclusions: Geomorphic and topographic evidence for classical LDA/LVF flow units emplaced along the dichotomy boundary are preserved in the Tanaica Montes region. The large-scale integration of their intriguing flow patterns reveals topography assisted emplacement of flow units in the downslope. Overall, we could infer that a widespread accumulation and preservation of ice/snow has occurred during the Late Amazonian over vast areas of the northern and southern mid-latitudes. Taken together, we infer the landscape evolution process as a combination of erosion, followed by cold-climate based degradation, accumulation/preservation of ice/snow during the late Amazonian, and emplacement of flow units as a result of debris-covered glaciation.

References: [1] Baker D. M. H. et al. (2010) *ICARUS*, 207, 186-209. [2] Sinha R. K. and Murty S. V. S. (2013) *Planet. Space. Sci.*, 86, 10-32. [3] Holt J. W. et al. (2008) *Science*, 322, 1235-1238. [4] Plaut J. J. et al. (2009) *Geophys. Res. Lett.*, 36, L02203. [5] Fassett C. I. et al. (2014) *Geology*, 42(9), 763-766. [6] Levy J. S. et al. (2014) *J. Geophys. Res.*, 119(10), 2188-2196. [7] Scott D. H. and Tanaka K. L. (1986) *Geological Survey (US)*. [8] Tanaka K. L. et al. (2014) *Planet. Space Sci.*, 95, 11-24. [9] Malin M. C. et al. (2007) *J. Geophys. Res.*, 112, E05S04. [10] Smith D. E. et al. (2001) *J. Geophys. Res.*, 106 (E10), 23689-23722. [11] Dickson J. L. et al. (2007) *ICARUS*, 188, 315-323. [12] Ivanov B. A. (2001) *Space Sci. Rev.*, 96, 87-104.